ORNL/TM-2018/959

An Uncertainty Quantification of the Computational Fluid Dynamics Solution to the Modeling of the Contact Point in a Wire-Wrapped Fuel Assembly

Marc-Olivier G. Delchini
Laura P. Swiler
Emilian P. Popov
William D. Pointer

August, 2018

OAK RIDGE NATIONAL LABORATORY
MANAGED BY UT-BATTELLE FOR THE US DEPARTMENT OF ENERGY

ORNL/TM-2018/959

Reactor and Nuclear Systems Division

An Uncertainty Quantification of the Computational Fluid Dynamics Solution to the Modeling of the Contact Point in a Wire-Wrapped Fuel Assembly

Marc-Olivier G. Delchini,
Laura P. Swiler,
Emilian P. Popov, and
William D. Pointer

Date Published: August, 2018

Prepared by
OAK RIDGE NATIONAL LABORATORY
Oak Ridge, TN 37831-6283
managed by
UT-Battelle, LLC
for the
US DEPARTMENT OF ENERGY
under contract DE-AC05-00OR22725

CONTENTS

LIST OF FIGURES iv
LIST OF TABLES v
ACRONYMS vi
ABSTRACT 1
1. INTRODUCTION 1
2. METHODOLOGY 3
3. Results and Analysis 5
3.1 FRICTION FACTOR 5
3.2 SURFACE-AVERAGED VORTICITY 6
3.3 INTERNAL MIXING PARAMETERS 6
4. VARIANCE-BASED SENSITIVITY ANALYSIS 8
5. CONCLUSIONS AND FUTURE WORK 10

LIST OF FIGURES

1 Schematic of a wire-wrapped pin bundle. 2
2 Closed-gap versus open-gap approach. 3
3 Zoomed-in view of the wire. 4
4 Interaction and interval plots for friction factor. 6
5 Friction factor as a function of Reynolds number for 1-, 7-, and 19-pin bundles. 7
6 Interaction and interval plots for surface-averaged vorticity. 8
7 Interaction and interval plots for internal mixing parameter. 8
8 Internal mixing parameters as a function of Reynolds number for 1-, 7- and 19-pin bundles. . 9
9 Sobol indices for friction factor (right) and relative error of the friction factor (left). 9
10 Sobol indices for mixing parameters (left) and vorticity (right) 10

LIST OF TABLES

1 Nominal geometric and flow parameters of a MYRRHA wire-wrapped pin bundle 2
2 Mesh indices 5
3 Input parameters sampled in Dakota input deck 5

ACRONYMS

BL	boundary layer
CAD	computer-aided design
CFD	computational fluid dynamics
DOE	US Department of Energy
MYRRHA	Multi-Purpose Hybrid Research Reactor for High-Tech Applications
NEAMS	Nuclear Energy Advanced Modeling and Simulation
RANS	Reynolds-Averaged Navier-Stokes
SA	sensitivity analysis
UQ	uncertainty quantification

ABSTRACT

An uncertainty quantification and sensitivity analysis of the turbulent flow in a wire-wrapped pin bundle to the contact-point model and the inlet conditions is presented. Three geometries are considered in this work that are an infinitely large bundle (single subchannel with periodic boundary conditions in the stream-wise direction), a 7-pin bundle and a 19-pin bundle. The response functions of this study are the friction factor, the vorticity and the mixing parameters. The results show that the friction factor is not sensitive to the contact-point model. The vorticity shows a strong dependency to the inclusion of prismatic layers near the wall boundaries. Results for the mixing parameters are inconclusive. A variance-based sensitivity analysis (Sobol indices) indicates that the influence of the contact-point model on the variance of the friction factor decreases when increasing the size of the bundle. Other response functions (vorticity and mixing parameters) show little sensitivity to the size of the bundle.

1. INTRODUCTION

In response to the objectives outlined by the US Department of Energy (DOE) Nuclear Energy Advanced Modeling and Simulation (NEAMS) program, an effort has been initiated to assess the applicability of a variety of thermal hydraulic analysis methods to predict the heat transfer and fluid dynamic phenomena associated with wire-wrapped bundle assemblies.

Modeling of three-dimensional flow in wire-wrapped pin bundles responds to at least two main constraints: (1) the turbulent nature of the flow (Reynolds numbers range from 40×10^3 to 65×10^3) and (2) the multiple contact points between helical-type wire spacers and pins (see Figure 1). Because of the complex flow features in the wire-wrapped bundle and the complex associated geometry, experimental and numerical studies are crucial for understanding the flow characteristics in subchannels of wire-wrapped bundles and for determining design limit parameters. With the recent development of intensive computing capabilities, numerical simulations of flow in wire-wrapped bundles were carried out using computational fluid dynamics (CFD) open-source and commercial packages [7, 2, 8, 4, 9]. Reynolds-averaged Navier-Stokes (RANS)–based simulations are commonly used to simulate flows in wire-wrapped bundle geometries because they require less computing resources than large eddy simulations while still sufficiently resolving the turbulent phenomena in this application. These studies allow for more detailed numerical investigations of turbulent flow in wire-wrapped bundles such as secondary flow and cross flow that are triggered by the helical-type wire spacer.

As previously stated, the multiple contact points between wires and pins make the computer-aided design (CAD) model and the mesh challenging to generate. The contact points can be divided into two categories when considering a cross section view of the bundle that is perpendicular to the stream-wise direction. The first category corresponds to the contact point between a pin and a wire wrapped around it. This is modeled by adding a fillet with a radius set to 5% of the wire radius. With this model, the contact point between the pin and the wire wrapped around it becomes a line in two dimensions and a surface in three dimensions. This can be effectively meshed. The second category of contact point is located between a wire and its adjacent pins. More explicitly, the wire is helically wrapped around a pin so that at most it touches six adjacent pins because of the triangular assembly pitch, resulting in six contact points. A similar approach to that described above can be used, but it is difficult to achieve since the contact point is localized. An analysis of the published literature reveals that two approaches are commonly used to overcome the complexity of meshing a contact point between adjacent pins and wires. The two approaches consist of either introducing a gap

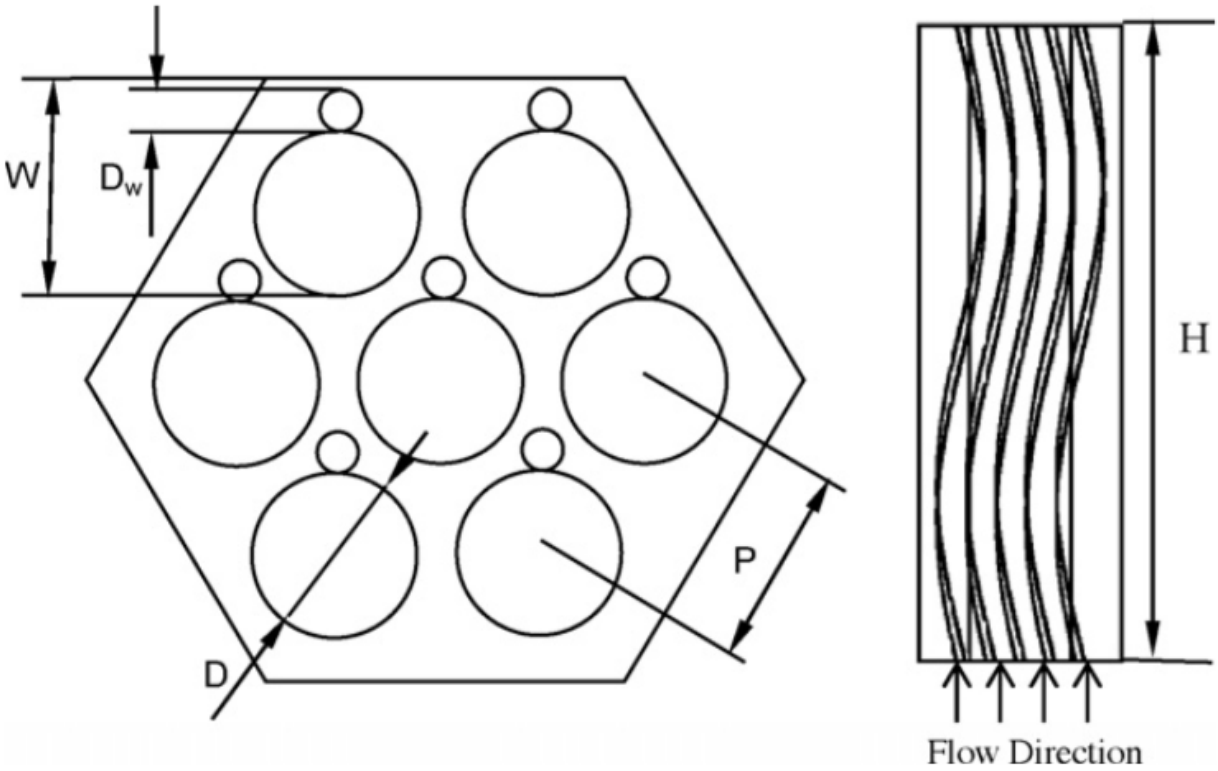

Figure 1. Schematic of a wire-wrapped pin bundle.

between the adjacent pin and the wire—referred to as an *open-gap approach* (Figure 2b) [8]—or embedding the wire to the adjacent pin—referred to as a *closed-gap approach* (Figure 2a) [5]. These two approaches seem to lead to reasonable predictions of pressure drops when compared with correlation and experimental data. However, there is a lack of comparative study between the open-gap and closed-gap approaches for wire-wrapped pin bundles. The sensitivity of a numerical solution of a turbulent flow to the contact-point model remains undefined. This paper investigates the sensitivity of the CFD numerical solution of an isothermal turbulent flow (lead-bismuth coolant) in the Multi-Purpose Hybrid Research Reactor for High-Tech Applications (MYRRHA), which is being designed and built at the SCK·CEN Belgian Nuclear Research Centre [9]. Its geometric and flow parameters are given in Table 1. Sensitivity to three

Table 1. Nominal geometric and flow parameters of a MYRRHA wire-wrapped pin bundle

Parameter	Value	Units
P	8.4	mm
H	262	mm
D_w	1.85	mm
D	6.55	mm
W	D+1.3D_w	mm
u_{inlet}	2.0	m/s
T_{inlet}	613.5	K

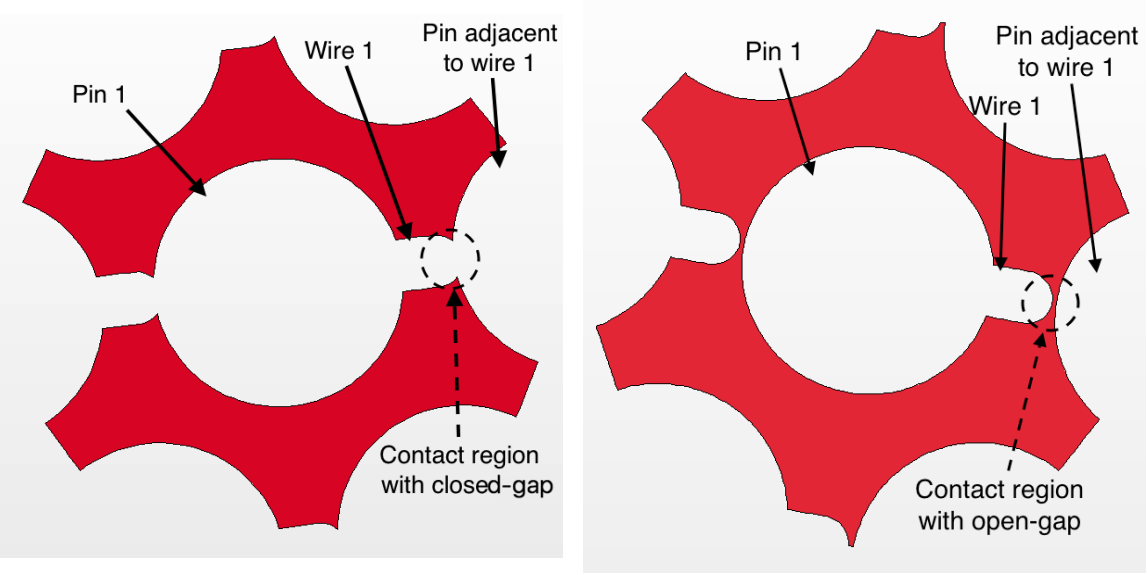

(a) Closed-gap model

(b) Open-gap model

Figure 2. Closed-gap versus open-gap approach.

contact-point models denoted as circular (C), trimmed (T), and elliptical (E) is studied (see Figure 3). Sensitivity analysis (SA) of the numerical solution to the insertion of boundary layers (BLs) along wall boundaries is also investigated. This paper also presents an uncertainty quantification (UQ) to the Reynolds number computed from inlet flow conditions. The output parameters or response functions of the study are the friction factor, vorticity, and mixing parameters [10]. Three bundles are considered in this paper: a single-pin bundle with periodic boundary conditions in the span-wire direction (equivalent to an infinite lattice), a 7-pin bundle, and a 19-pin bundle.

2. METHODOLOGY

RANS simulations were carried out in this study using the STAR-CCM+ commercial CFD package. STAR-CCM+ is a finite volume method code used to simulate heat and mass transport at the continuum scale. The numerical solution was obtained using the SIMPLE algorithm with Rhie-Chow interpolation for velocity-to-pressure coupling and is accelerated with algebraic, multigrid preconditioning. Energy-to-flow coupling is treated using a split operator methodology. The liquid metal coolant is treated as incompressible, and the Shear-Stress Transport K-Omega turbulence model is used with a two-layer all y+ wall function. The geometry is meshed with polyhedral elements. Wall boundary conditions are applied to wires, pins, and the hexagonal shell, while inlet and outlet boundary conditions are applied in the stream-wise direction. A convergence study which included comparison to the Chen-Todreas correlation of the friction factor revealed that a base element size of 1 mm was optimal to ensure accuracy and convergence of the numerical solution within reasonable CPU time. Six meshes are generated for each bundle: one for each contact-point model (E, C, and T) meshed with and without the BLs option.

The UQ and SA Dakota package [1] is used to drive STAR-CCM+, to feed the STAR-CCM+ input deck with input parameters through the Perl dprepo script (provided by Dakota), and to collect response functions from

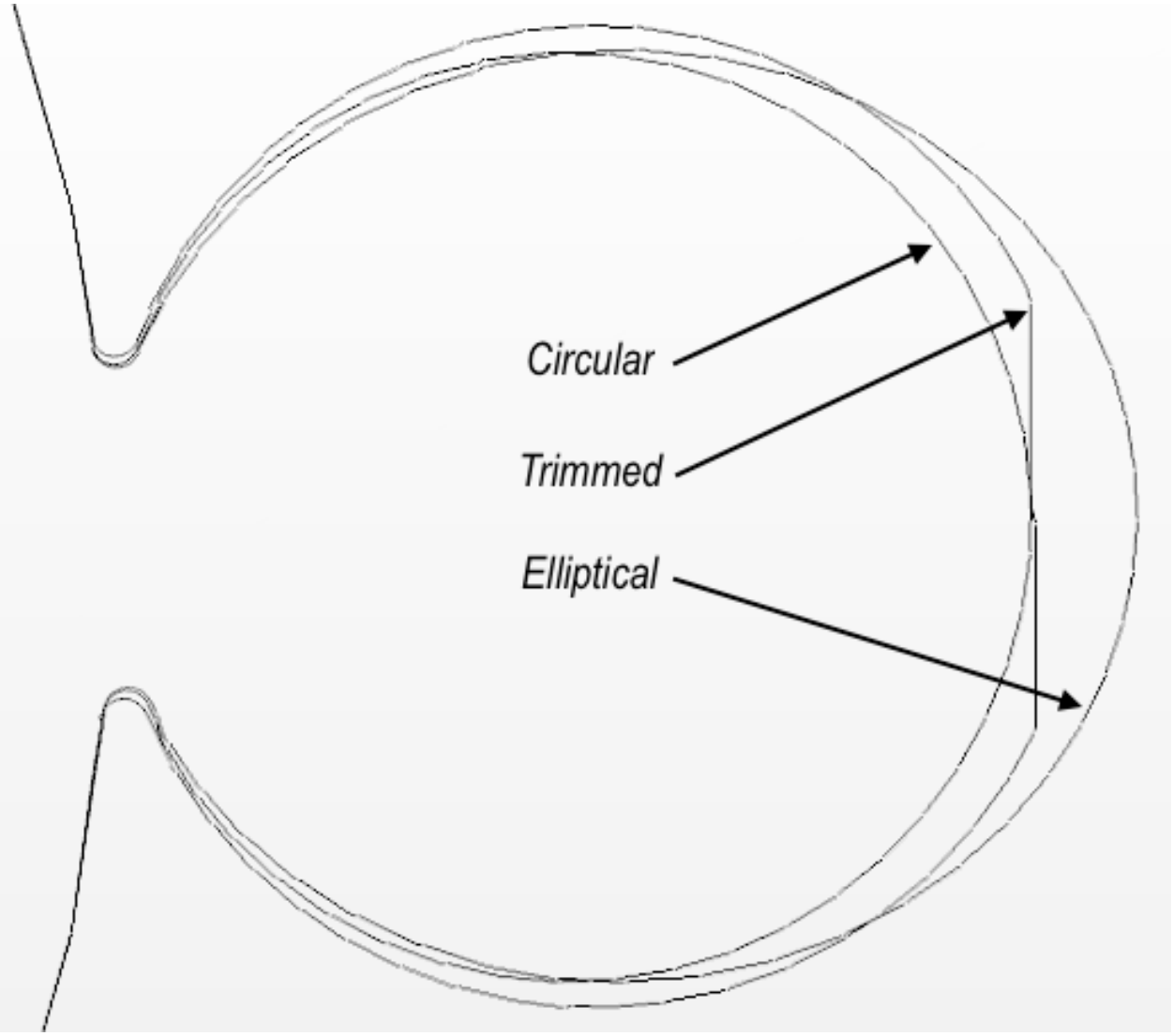

Figure 3. Zoomed-in view of the wire.

each run. The Dakota input deck samples five input parameters, which are displayed in Table 3. The statistical method chosen for this study is the Latin Hypercube sampling method with 250 samples. The mesh indices are related to the contact-point model and the insertion of BLs, as detailed in Table 2. The response functions are the friction factor, the surface-averaged vorticity, and the mixing parameters. The friction factor is obtained from the pressure drop and the hydraulic diameter D_h that are numerically computed in STAR-CCM+. The vorticity is surface averaged over a cross sectional area of the bundle perpendicular to the stream-wise direction and halfway between the inlet and outlet boundaries. The internal mixing parameter as defined in [3] is post-processed using the formula given in Eq. 1:

$$\epsilon_{internal} = \frac{transverse\ mass\ flux}{bundle\ axial\ mass\ flux} \tag{1}$$

Table 2. Mesh indices

Mesh indices	Contact-point model	Gap	Boundary layers
1	Circular wire	Yes	No
2	Circular wire	Yes	Yes
3	Elliptical wire	No	No
4	Elliptical wire	No	Yes
5	Trimmed wire	Yes	No
6	Trimmed wire	Yes	Yes

Table 3. Input parameters sampled in Dakota input deck

Parameter name (float)	Distribution type	Mean value	σ (10 % uncertainty)
u_{inlet}	normal_uncertain	2.0 m/s	0.066
T_{inlet}	normal_uncertain	613.5 K	20.24
ρ_{mult}	normal_uncertain	1.0	0.002667
μ_{mult}	normal_uncertain	1.0	0.002667
Parameter name	Distribution type	Values	Probability associated with each value
mesh index (integer)	histogram_point_uncertain	1, 2, 3, 4, 5, 6,	0.14, 0.21, 0.10, 0.15, 0.16, 0.24

3. Results and Analysis

This section presents results and analyses of the UQ and SA studies of a turbulent flow in 1-, 7-, and 19-pin bundles. For the purpose of this study and without loss of generality, the input parameters of Table 3 can be grouped into two parameters: the hydraulic diameter-based Reynolds number Re_{D_h} and the mesh index. Responses of the friction factor, the surface-averaged vorticity, and the internal mixing parameter to the sampling of the Reynolds number and the mesh index are investigated in the following three subsections. For each response function, the interaction and interval plots as a function of the mesh are shown and commented. Variations with respect to the Reynolds number are also presented when relevant. All 250 runs successfully converged to a steady-state solution; thus, all were included to generate the plots shown herein. A measurement uncertainty of 10 % was chosen for the velocity and the temperature inlet quantities.

3.1 FRICTION FACTOR

Plots of the interval and interaction of the friction factor as a function of the mesh index are shown in Figures 4a and 4b. In Figure 4a, the mean of the friction factor is plotted as a function of the mesh type with associated confidence intervals. The variations of the mean are within 5% when changing the mesh type, and the confidence intervals overlap. This suggests that the mean friction factors predicted by the different mesh types belong to the same population. In other words, the contact-point model and the insertion of BLs at the wall boundaries do not strongly affect the friction factor. Figure 4b displays the mean friction factor as a function of the mesh index for each bundle type (i.e., 1-, 7-, and 19-pin bundles). This strengthens the previous findings that the mean friction factor is not sensitive to the mesh index for all geometries. Figure 5 shows the variations of the friction factor as a function of the Reynolds number for all geometries and for all meshes. The figure illustrates that the friction factor decreases as the Reynolds number increases, as

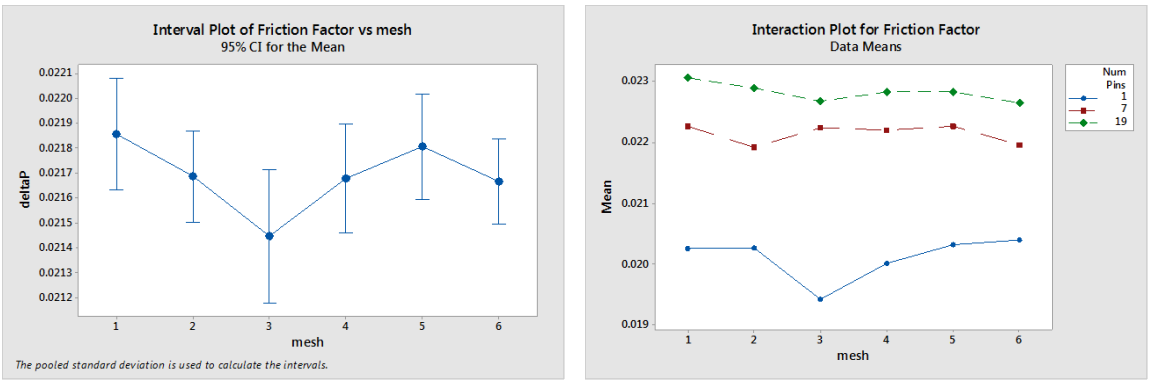

(a) Interval plot **(b) Interaction plot**

Figure 4. Interaction and interval plots for friction factor.

predicted by the correlations [10, 6]. This behavior is independent of the mesh type or the geometry. For a given geometry, the variation of the friction factor is within 5% of the mean value.

3.2 SURFACE-AVERAGED VORTICITY

Next, the results of the surface-averaged vorticity as a function of the mesh index are presented and analyzed. The interval and interaction plots of the surface-averaged vorticity are displayed in Figures 6a and 6b, respectively. The variations of the vorticity with respect to the mesh type are similar over the different geometries: the meshes with BLs predict a surface-averaged vorticity that is 50–100% higher than that predicted by meshes without BLs. The confidence interval displayed in Figure 6a shows that even and odd mesh indices belong to two distinct populations. The same conclusions are drawn by studying variations of the surface-averaged vorticity for each geometry. Unlike the friction factor results, these results suggest that the accuracy of the numerical solution next to the wall boundaries strongly affects the vorticity, which is tied to the performance of the turbulent model.

3.3 INTERNAL MIXING PARAMETERS

The last response function of interest for this study is the internal mixing parameter. Results as a function of the mesh type are presented herein. In Figure 7b, it is observed that the mixing parameter values predicted for the 1-pin bundle are positive and much larger than for the other geometries. One explanation for this result could be the periodic boundary conditions set in the span-wise direction of the mesh for the 1-pin bundle that enhance mixing. For the 7- and 19-pin bundle cases, the mean values of the internal mixing parameters are either positive or negative. It is difficult to draw a clear conclusion about the sensitivity of the internal mixing parameter with respect to the contact-point model and the insertion of BLs. The change of sign in the mixing parameter suggests that the flow direction is dependent of the mesh index. Also, since the bundle cases considered for this study are small, the internal subchannels are not sufficiently shielded from the edge and corner subchannels, so their influence cannot be neglected. Results presented in Figure 7a are somewhat misleading, as the confidence intervals overlap, suggesting that all mesh indices belong to the

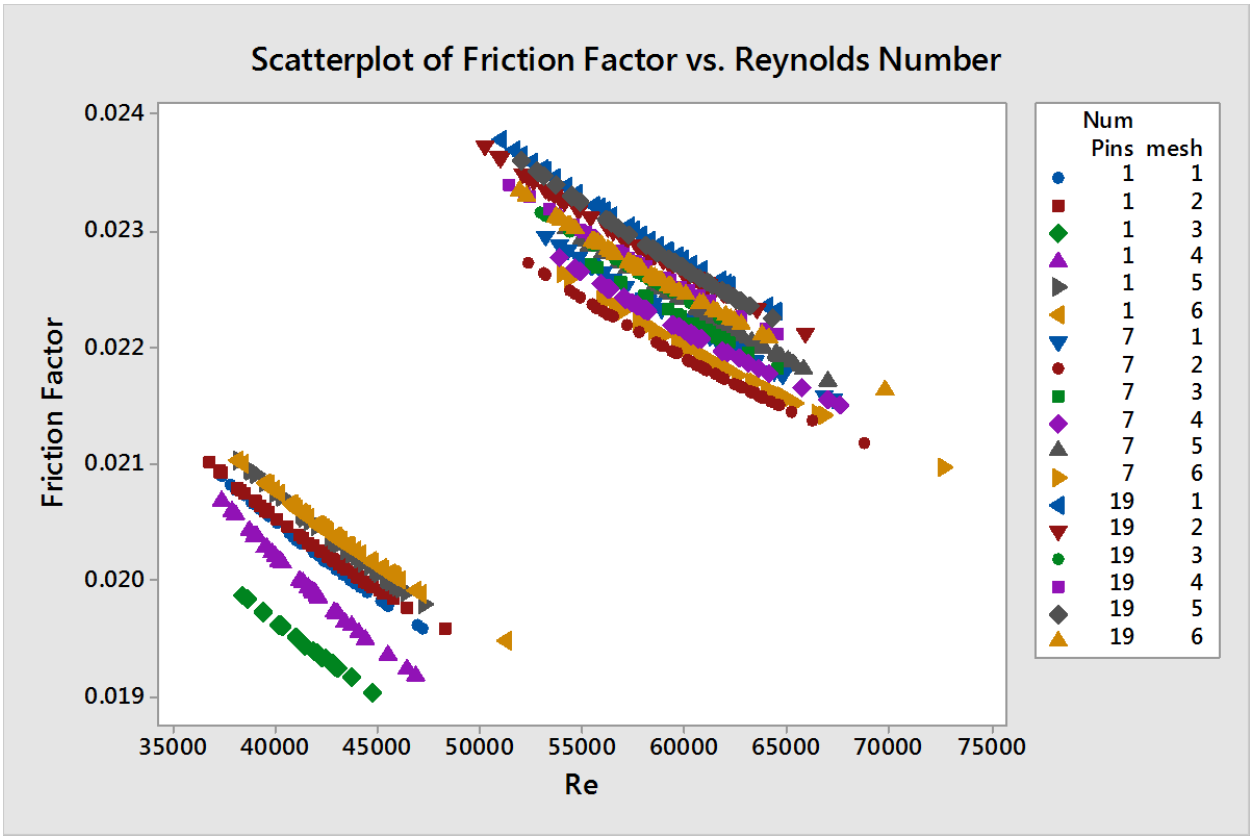

Figure 5. Friction factor as a function of Reynolds number for 1-, 7-, and 19-pin bundles.

same population. This is explained by the large values of the mixing parameter for the 1-pin bundle case that dominate the mixing parameter values predicted for the 7- and 19-pin bundle cases.

The internal mixing parameter as a function of the Reynolds number is shown in Figure 8 for all 250 runs. Experimental data and the Cheng-Todreas correlation suggest that the mixing parameters are independent of the Reynolds number, which is consistent with the numerical results presented in Figure 8a. Figure 8b shows that, unlike the 1-pin bundle geometry, mixing parameters predicted for the 7- and 19-pin geometries have a nonconstant sign. Mixing parameters obtained with an open-gap approach are always negative except for the cases corresponding to the 7- and 19-pin bundles with mesh type 2. Mixing parameters obtained with the closed-gap approach are always positive except for the case corresponding to the 7-pin bundle with mesh type 3.

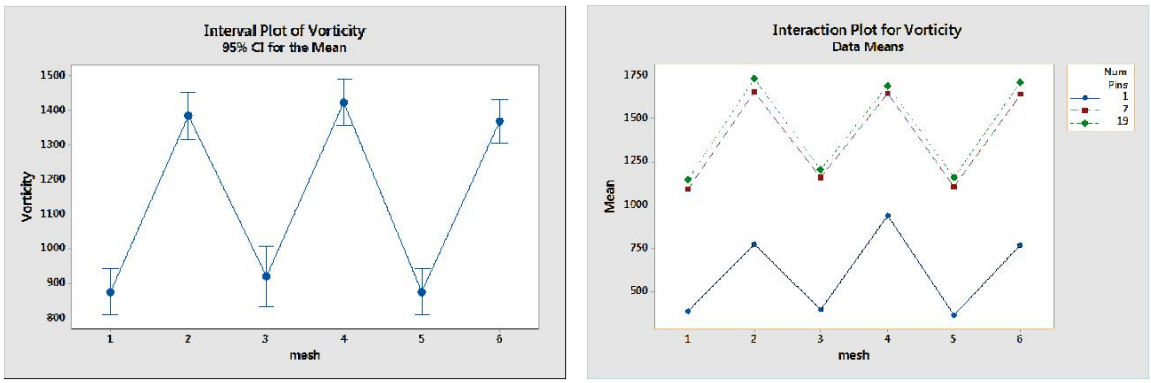

(a) Interval plot **(b) Interaction plot**

Figure 6. Interaction and interval plots for surface-averaged vorticity.

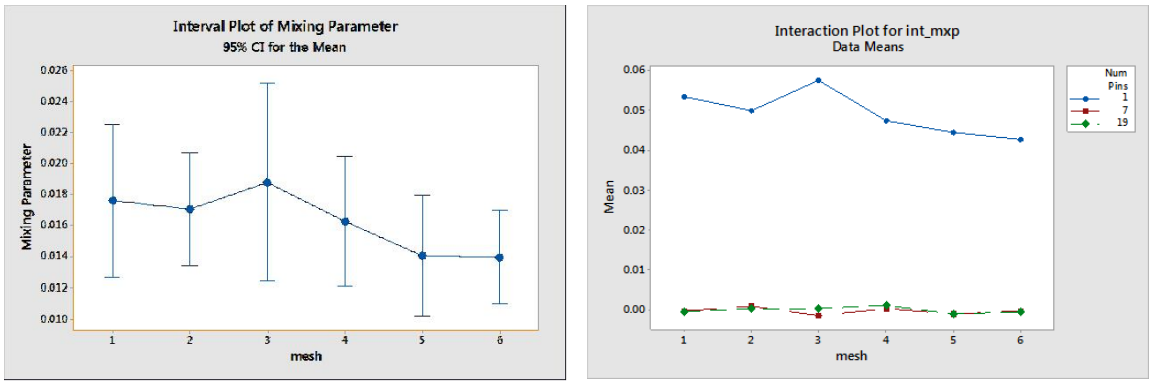

(a) Interval plot **(b) Interaction plot**

Figure 7. Interaction and interval plots for internal mixing parameter.

The current results do not provide adequate data to draw a conclusion on the sensitivity of the internal mixing parameters to the mesh index. Further data from larger pin-bundles would be required to minimize the influence of the edge and corner subchannels on the internal subchannel.

4. VARIANCE-BASED SENSITIVITY ANALYSIS

This section presents results of a variance-based sensitivity analysis, which is also referred to as the *Sobol method*. The main idea of this method is to decompose the output variance into the contributions associated with each input factor by computing Sobol indices. For example, given a model with two inputs and one output, one might find that 70% of the output variance is caused by the variance in the first input and 30% by the variance in the second.

Sobol indices were computed for each of the outputs, including the friction factor, the relative error of the friction factor, the mixing parameters, and the vorticity. Plots of the Sobol indices for all geometries (1-, 7-, and 19-pin bundles) are shown in Figures 9–10b. The labels on the horizontal axes range from 1 to 5 and correspond to the different input variables, including the velocity, the temperature, the viscosity, the density,

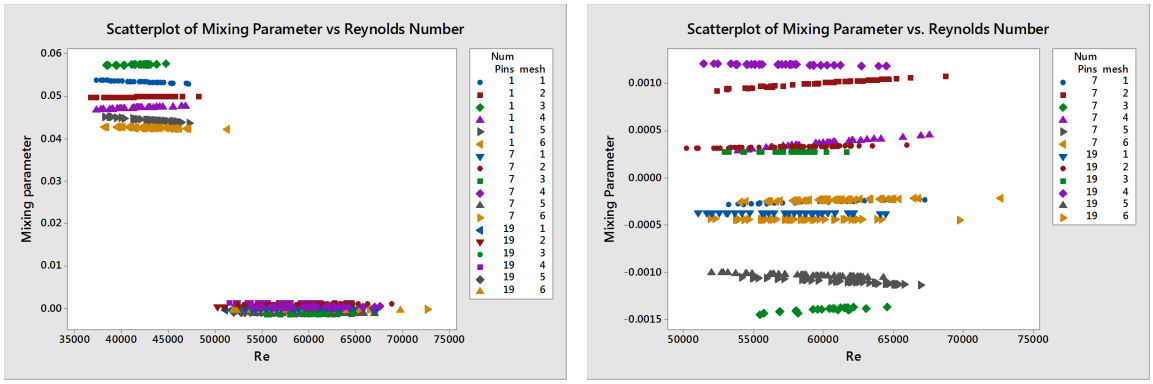

(a) Results for all geometries **(b) Results for 7- and 19-pin bundle geometries.**

Figure 8. Internal mixing parameters as a function of Reynolds number for 1-, 7- and 19-pin bundles.

and the mesh, respectively.

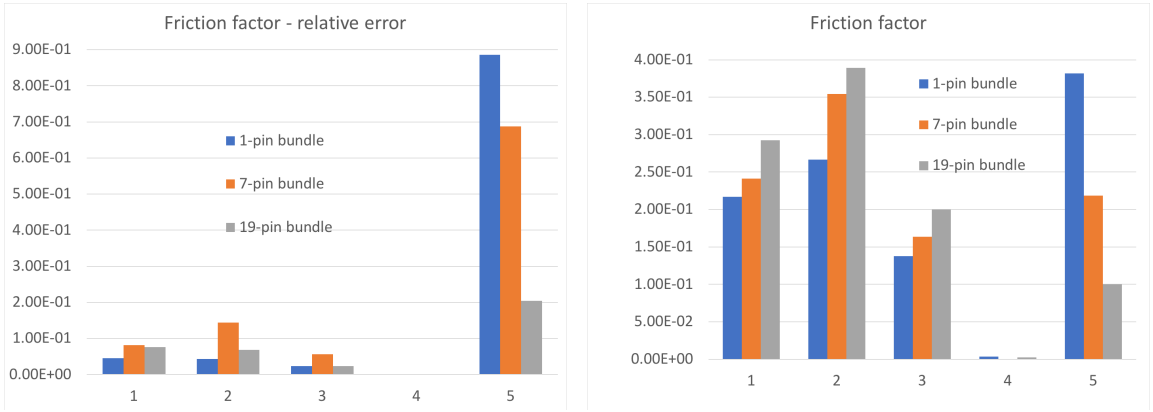

(a) **(b)**

Figure 9. Sobol indices for friction factor (right) and relative error of the friction factor (left).

The relative error of the friction factor was computed by using the Chen-Todreas correlation as a reference. The corresponding Sobol indices show that the relative error is very sensitive to the variance in the contact-point model (index 5). Other variables have a limited effect on the relative error. The Sobol indices for the friction factor are shown in Figure 9b, indicating a more uniform sensitivity to all inputs except the density (index 4). Note that the sensitivity of the friction factor to the variance in the contact-point model decreases as the number of pins increases. Other inputs (indices 1–4) show the opposite behavior. This suggests that the influence of the contact-point model on the variance of the friction factor decreases when increasing the size of the bundle, i.e., the number of pins. The Sobol indices of the mixing parameters presented in Figure 10a clearly show a strong sensitivity to the mesh (index 5) and very little sensitivity to all other inputs (Sobol indices are below 10^{-4} for inputs 1–4). The variance-based sensitivity analysis for the vorticity shows the same behavior as for the mixing parameters, as displayed in Figure 10b. The Sobol indices of both the vorticity and the mixing parameters show little sensitivity to the number of pins in the bundle.

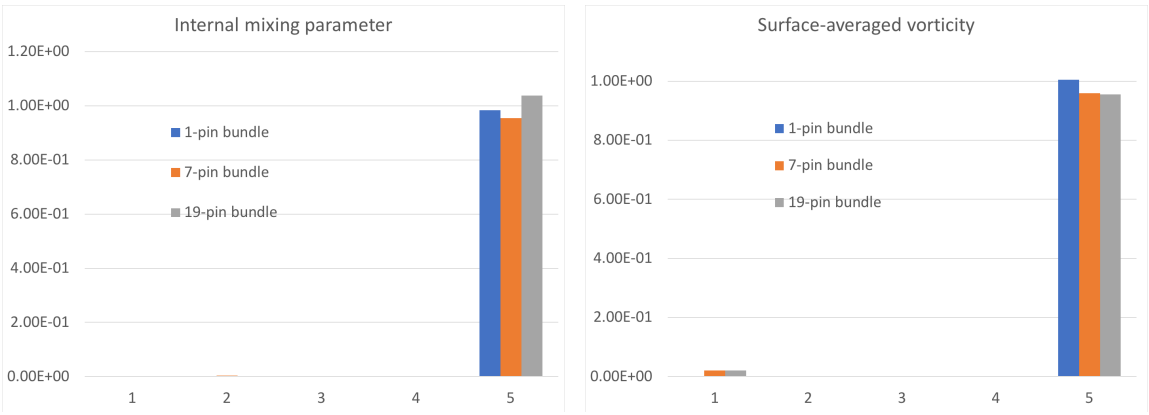

(a) Sobol indices for mixing paramaters. **(b) Sobol indices for vorticity.**

Figure 10. Sobol indices for mixing parameters (left) and vorticity (right) .

5. CONCLUSIONS AND FUTURE WORK

This paper presents a UQ and SA analysis of a turbulent flow in wire-wrapped pin bundles and attempts to draw conclusions on the effect of the Reynolds number, the contact-point model, and the insertion of BLs on the three response functions of friction factor, internal mixing parameters, and surface-averaged vorticity. Results show that the friction factor is not sensitive to the contact-point model or the inclusion of BLs on wall boundaries. In other words, the friction factor is correctly predicted by all mesh types for all bundle cases. Study of the variation of the surface-averaged vorticity shows a strong dependence on the insertion of BLs; meshes with BLs predict a higher vorticity than meshes without BLs. This is of interest, as the vorticity is tied to the turbulent model. The variation of the mixing parameters does not lead to any meaningful conclusions: this is believed to be caused by the too-large influence of the edge and corner subchannels, which is characteristic of small bundles.

A variance-based sensitivity study was also performed by computing the Sobol indices for each of the response functions. It was found that the sensitivity of the friction factor to the variance in the mesh decreases as the number of pins increases, and the variance of the friction factor's relative error is mostly caused by the variance in the mesh. The Sobol indices computed for the mixing parameters and vorticity also show a large sensitivity to the variance of the mesh.

Future work will focus on identifying other response functions of interest and will investigate larger pin bundles.

References

[1] B M Adams, L E Bauman, W J Bohnhoff, K R Dalbey, M S Ebeida, J P Eddy, M S Eldred, P D Hough, K T Hu, J D Jakeman, J A Stephens, L P Swiler, D M Vigil, and T M Wildey. Dakota, a multilevel parallel object-oriented framework for design optimization, parameter estimation, uncertainty quantification, and sensitivity analysis: Version 6.0 users manual. Technical report, Sandia National Laboratories, SAND2014-4633, July 2014.

[2] A Ahmad and K-Y Kim. Three-dimensional analysis for flow and heat transfer in a wire-wrapped fuel assembly. In *Proc. of ICAPP 2005*, Seoul, Korea, 2005.

[3] S.K. Chen, N.E. Todreas, and N.T. Nguyen. Evaluation of existing correlations for the prediction of pressure drop in wire-wrapped hexagonal array pin bundles. *Nuclear Engineering Design*, 267:109–131, 2014.

[4] P Fisher, J Lottes, and A Siegel. Large Eddy Simulation of Wire-Wrapped Fuel Pins I: Hydrodynamics in a Periodic Array. In *Joint International Topical Meeting on Mathematics & Computation and Supercomputing in Nuclear Applications*, Monterey, California, USA, 2007.

[5] J-H Jeong, J Yoo, K-L Lee, and K-S Ha. Three-dimensional flow phenomena in a wire-wrapped 37-pin fuel bundle for sfr. *Nucl Eng Technol*, 47(5):523–533, 2015.

[6] E H Novendstern. Turbulent flow pressure drop model for fuel rod assemblies utilizing a helical wire-wrap spacer system. *Nuclear Engineering and Design*, 92:19–27, 1972.

[7] D W Pointer, P Fisher, and A Siegel. RANS-based CFD Simulations of Wire-Wrapped Fast Reactor Fuel Assemblies. In , Anaheim, CA, USA, 2008.

[8] W. D. Pointer, J. Smith, A. Siegel, and P. Fisher. Rans simulations of turbulent diffusion in wire-wrapped sodium fast reactor fuel assemblies. In *Proc. FR09*, Kyoto, Japan, Nov. 2009.

[9] A Shams, F Roelofs, and E M J Komen. High-Fidelity Numerical Simulation of the Flow through an Infinite Wire-Wrapped Fuel Assembly. In *16th International Conference on Nuclear Reactor Thermal Hydraulics (NURETH-16)*, Chicago, Illinois, USA, 2015.

[10] N.E. Todreas and S.K. Cheng. Hydrodynamic models and correlations for bare and wire-wrapped hexagonal rod bundles - bundle friction factors, subchannel friction factors and mixing parameters. *Nuclear Engineering and Design*, 92:227–251, 1985.